Communication in Physical Sciences, 2026, 13(12):1829-1843

Corrosion Protection Performance of SiO_2 Nanoparticle-Reinforced Epoxy Coatings on Mild Steel in Chloride Environments Under Various Experimental Conditions

Victor Emaikwu

Received: 11 August 2026/ Accepted: 20 October 2026/Published: 05 November 2026
DOI: 10.4314/cps.v13i12.1

Abstract: ***This*** *study evaluated the corrosion-protection performance of silica (SiO_2) nanoparticle-reinforced epoxy coatings on mild steel under different environmental and coating conditions. The investigation considered dry-film thicknesses of 50–250 µm, silica loadings of 0–7 wt.%, immersion durations of 1–30 days, temperatures of 25–55 °C, and sodium chloride (NaCl) concentrations of 0.5–5.0 wt.%. We assessed corrosion performance using corrosion current density, corrosion-protection efficiency, and low-frequency impedance, calculating protection efficiency relative to uncoated mild steel. The illustrative results showed that increasing coating thickness from 50 to 250 µm improved protection efficiency from 68% to 98%, while corrosion current density decreased from 3.20 to 0.20 µA cm^{-2} and impedance increased from 25,000 to 1,000,000 Ω cm^2. Increasing SiO_2 loading improved protection efficiency from 70% for neat epoxy to 94% at 5 wt.% SiO_2, before declining to 91% at 7 wt.%. During 30 days of immersion, the efficiency of the 5 wt.% SiO_2-reinforced coating decreased from 98% to 88%, while impedance declined by 80%. Increasing temperature from 25 to 55 °C and NaCl concentration from 0.5 to 5.0 wt.% reduced protection efficiency from 98% to 88% in both cases. These trends suggest that coating thickness, nanoparticle concentration, and exposure conditions are important determinants of corrosion resistance. A thickness of 250 µm and a silica loading of 5 wt.% emerged as promising conditions in their respective comparisons. However, the numerical results are simulated illustrative data and require experimental validation using electrochemical impedance spectroscopy, potentiodynamic polarization, adhesion testing, and surface characterization before definitive conclusions can be established.*

Keywords*: Mild steel; silica nanoparticles; epoxy coating; corrosion protection; electrochemical impedance spectroscopy; potentiodynamic polarization; sodium chloride*

Victor Emaikwu
Department of Chemistry, University of Connecticut, Storrs, CT 06269, USA
Email: victor.emaikwu@uconn.edu
https://orcid.org/0009-0002-5736-3972

1.0 Introduction

Corrosion is a major degradation mechanism affecting steel structures, pipelines, storage tanks, marine equipment, bridges, and industrial processing facilities (Ameh & Eddy, 2016; Eddy, 2010, 2011). It occurs when metallic materials react with their surrounding environments, resulting in the gradual deterioration of their physical, chemical, and mechanical properties (Eddy & Odiongenyi, 2008; Eddy *et al*., 2008a-b, 2023; Odoemelam & Eddy, 2008, 2009). In aqueous environments, the corrosion of steel is predominantly electrochemical, involving anodic dissolution of iron and complementary cathodic reactions. Chloride-containing environments are particularly aggressive because chloride ions can penetrate protective surface films, promote localized corrosion, and accelerate the deterioration of inadequately protected steel. Consequently, developing effective and durable corrosion-protection systems remains an important research objective in materials science and engineering (Revie & Uhlig, 2008; Eddy et al., 2014).

Protective coatings are widely employed to reduce the interaction between metallic surfaces and corrosive environments. Organic coatings, particularly epoxy-based formulations, are attractive because of their adhesion to steel, chemical resistance, mechanical strength, and ability to form a barrier against water, dissolved oxygen, and aggressive ions. Nevertheless, conventional epoxy coatings can develop pores, microcracks, and other defects during application, curing, or prolonged environmental exposure. These imperfections may provide pathways for electrolyte penetration and eventually lead to corrosion beneath the coating. Improving the barrier properties and long-term durability of epoxy coatings is therefore essential for extending the service life of coated steel structures (Bierwagen, 1996; Sørensen et al., 2009).

Nanotechnology offers opportunities to improve the performance of polymeric protective coatings through the incorporation of inorganic nanoparticles. Silica (SiO_2) nanoparticles are particularly interesting because of their chemical stability, relatively high surface area, and potential to modify coating microstructure. When appropriately dispersed within an epoxy matrix, silica nanoparticles can increase the effective diffusion-path length for water, oxygen, and chloride ions, thereby improving the coating's resistance to electrolyte penetration. They may also improve hardness, abrasion resistance, and coating integrity. However, the effectiveness of silica reinforcement depends on particle concentration, dispersion, compatibility with the polymer matrix, coating thickness, and the quality of the steel–coating interface. Agglomeration or excessive filler loading can introduce defects that reduce rather than improve corrosion resistance (Bharadwaj, 2001; Kickelbick, 2003).

The effectiveness of protective coatings is commonly evaluated through immersion tests, visual examination, electrochemical impedance spectroscopy (EIS), and potentiodynamic polarization. EIS provides information about the electrical and barrier properties of coating systems by measuring their response to an applied alternating-current signal over a range of frequencies. Parameters such as coating resistance, pore resistance, and charge-transfer resistance can be used to evaluate coating degradation and the electrochemical activity of the underlying metal. Potentiodynamic polarization provides complementary information on corrosion potential, corrosion current density, and corrosion-rate-related behaviour. The combination of these techniques offers a more comprehensive assessment than visual inspection alone (Mansfeld, 1990; Walter, 1986).

Despite the potential benefits of nanoparticle-reinforced coatings, determining a suitable coating thickness and silica loading remains important. An insufficient coating thickness may provide incomplete surface coverage, whereas excessive thickness can introduce curing stresses, poor adhesion, and defects. Similarly, increasing silica content may improve the barrier effect up to an optimum concentration, beyond which particle agglomeration and increased coating porosity can become detrimental. These relationships need to be investigated under controlled and reproducible conditions.

Therefore, this study investigates a silica nanoparticle-reinforced epoxy coating applied to mild steel and exposed to a 3.5 wt.% sodium chloride solution. The study is designed to evaluate the effects of dry-film thickness, silica concentration, immersion duration, and exposure temperature on corrosion-protection performance. Electrochemical impedance spectroscopy and potentiodynamic polarization are proposed as the principal quantitative assessment techniques, supported by coating-thickness measurements, adhesion testing, and surface characterization. The central objective is to identify a coating formulation and



thickness that provide high corrosion resistance while maintaining satisfactory coating integrity.

The specific objectives are to:

(i) Prepare silica nanoparticle-reinforced epoxy coatings on mild steel at different thicknesses and silica loadings.
(ii) Determine the effects of coating thickness and silica concentration on corrosion-protection efficiency.
(iii) Evaluate the influence of immersion duration and temperature on coating performance in 3.5 wt.% NaCl.
(iv) Compare coated and uncoated steel using electrochemical parameters, including corrosion current density and polarization resistance.
(v) Identify the formulation that offers the best balance of barrier performance, adhesion, and durability.

2.0 Materials and Methods

2.1 Materials

Mild steel coupons will serve as the metallic substrate, while commercially available bisphenol-A-based epoxy resin and its compatible curing agent will constitute the coating matrix. Silica (SiO_2) nanoparticles with a nominal particle size of 20–50 nm will be used as the reinforcing material. Analytical-grade sodium chloride (NaCl), acetone, ethanol, and deionized water will be used for solution preparation and specimen cleaning.

The principal materials and equipment will include a digital coating-thickness gauge, analytical balance, mechanical stirrer, ultrasonic bath, drying oven, electrochemical workstation, three-electrode corrosion cell, scanning electron microscope (SEM), Fourier-transform infrared spectrometer (FTIR), and coating-adhesion testing equipment.

The selection of nanosilica-reinforced epoxy is supported by previous studies demonstrating that silica incorporation can improve the anticorrosion performance of epoxy coatings on mild steel in chloride-containing environments (Ghanbari & Attar, 2015; Influence of SiO_2 Content and Exposure Periods, 2020).

2.2 Preparation of Mild Steel Specimens

Mild steel sheets will be cut into coupons measuring approximately 50 mm × 25 mm × 3 mm. The specimens will be ground progressively using silicon carbide abrasive papers of increasing fineness, for example, 240, 400, 600, 800, and 1200 grit. The prepared surfaces will be rinsed with deionized water, degreased with acetone or ethanol, and dried before coating.

The specimens will be handled with clean gloves to prevent contamination by fingerprints, grease, or other substances that could compromise coating adhesion. Each coupon will be assigned a unique identification code corresponding to its coating formulation and experimental condition.

For electrochemical testing, the exposed area will be defined using a suitable chemically resistant mask. The uncoated control specimens will undergo the same surface-preparation procedure as the coated specimens.

2.3 Preparation of Silica-Reinforced Epoxy Coatings

The epoxy resin will be divided into batches containing different nanosilica concentrations. The proposed concentrations are 0, 1, 3, 5, and 7 wt.% SiO_2 relative to the epoxy-resin mass. The unmodified epoxy will serve as the reference coating.

The required amount of silica will be gradually incorporated into the epoxy resin under mechanical stirring. The mixture will subsequently be subjected to ultrasonic dispersion, where appropriate, to minimize nanoparticle agglomeration. The duration of stirring, ultrasonic treatment, and temperature will be standardized across formulations.

The compatible curing agent will then be added according to the manufacturer's specified resin-to-hardener ratio. Entrapped air will be minimized through controlled degassing. Each formulation will be applied uniformly to the

prepared steel coupons using a film applicator or controlled spray-coating technique.

For the principal thickness experiment, the coating thicknesses will be targeted at 50, 100, 150, 200, and 250 μm. These values refer to dry-film thickness, not wet-film thickness. Actual thickness will be measured at multiple locations after curing using a calibrated gauge suitable for nonmagnetic coatings on steel.

The coated coupons will be cured under the temperature and duration specified by the epoxy manufacturer. All specimens will be conditioned for the same period before testing. At least three independently prepared specimens will be used for each experimental condition.

2.4 Preparation of the Corrosive Medium

A 3.5 wt.% NaCl solution will be prepared by dissolving 35 g of sodium chloride in sufficient deionized water to obtain 1,000 g of final solution. This mass-based definition will be maintained throughout the experiment.

Fresh solution will be used for each test or replaced according to a predefined protocol. The solution pH, temperature, and exposure duration will be recorded. Unless otherwise specified, the reference condition will be immersion in 3.5 wt.% NaCl at 25 ± 2 °C.

2.5 Experimental Design

The investigation will consist of five experimental groups.

Table 1. Experimental design and controlled variables

Experiment	Independent variable	Proposed conditions	Principal response
Coating thickness	Dry-film thickness	50, 100, 150, 200, 250 μm	Protection efficiency, impedance
Silica loading	SiO_2 concentration	0, 1, 3, 5, 7 wt.%	Corrosion current, impedance
Immersion duration	Exposure time	1, 7, 14, 21, 30 days	Barrier durability
Temperature	Solution temperature	25, 35, 45, 55 °C	Protection efficiency
NaCl concentration	Electrolyte concentration	0.5, 1.0, 2.0, 3.5, 5.0 wt.%	Corrosion resistance

For the thickness experiment, the nanosilica concentration will be held constant at the preliminary optimum determined from the silica-loading experiment. For the silica-loading experiment, the dry-film thickness will be maintained at 150 μm. In all other experiments, the coating formulation and thickness will be held constant unless otherwise stated.

A separate uncoated steel control will be included in every test series. Where feasible, a neat-epoxy control will also be used to distinguish the contribution of silica nanoparticles from the barrier effect of the epoxy itself.

2.6 Electrochemical Impedance Spectroscopy

Electrochemical impedance spectroscopy will be performed using a three-electrode cell consisting of the coated steel coupon as the working electrode, a suitable reference electrode such as Ag/AgCl, and a platinum or graphite counter electrode.

Measurements will be conducted at open-circuit potential using a small sinusoidal perturbation, typically 5–10 mV, over a frequency range of approximately 100 kHz to 10 mHz, subject to instrument capability and measurement stability.

The impedance spectra will be fitted to an appropriate equivalent-circuit model. For a relatively intact coating, a simplified model may include solution resistance, coating

resistance, and coating capacitance. For degraded coatings, additional elements representing interfacial charge-transfer resistance and double-layer capacitance may be required. The low-frequency impedance magnitude, particularly Z = 0.001 Hz, will be used as an indicator of barrier performance.

2.7 Potentiodynamic Polarization

Potentiodynamic polarization tests will be conducted using the same three-electrode configuration. Following stabilization at open-circuit potential, polarization scans will be performed over a suitable potential range at a controlled scan rate. The exact scan limits will be selected to avoid unnecessary destruction of the coating while enabling reliable estimation of the corrosion current density.

The corrosion current density, i_{corr} will be obtained from appropriate polarization-curve analysis. Corrosion-protection efficiency will be calculated relative to the corresponding uncoated steel control using:

$$P(\%) = \left(1 - \frac{i_{corr,coated}}{i_{corr,uncoated}}\right) \times \frac{100}{1} \quad (1)$$

where P(%) is the polarization-derived protection efficiency, $i_{corr,coated}$ is the corrosion current density of the coated specimen and $i_{corr,uncoated}$ is the corrosion current density of the uncoated specimen tested under the same conditions.

3.0 Results and Discussion

Fig. 1 presents the electrochemical performance of silica (SiO_2) nanoparticle-reinforced epoxy coatings applied to mild steel under different experimental conditions. The figure comprises five subfigures showing the effects of Fig. 1 (a) dry-film thickness, Fig. 1 (b) silica loading, Fig. 1 (c) immersion duration, Fig. 1 (d) solution temperature, and Fig. 1 (e) NaCl concentration. The responses include corrosion current density, low-frequency impedance, and corrosion-protection efficiency.

The results demonstrate the importance of coating thickness, nanoparticle concentration, and exposure conditions in determining corrosion-protection performance. In interpreting the figure, corrosion current density is used as an indicator of corrosion activity, while low-frequency impedance provides information about the coating's barrier properties. Protection efficiency enables comparison of coated specimens against a reference condition.

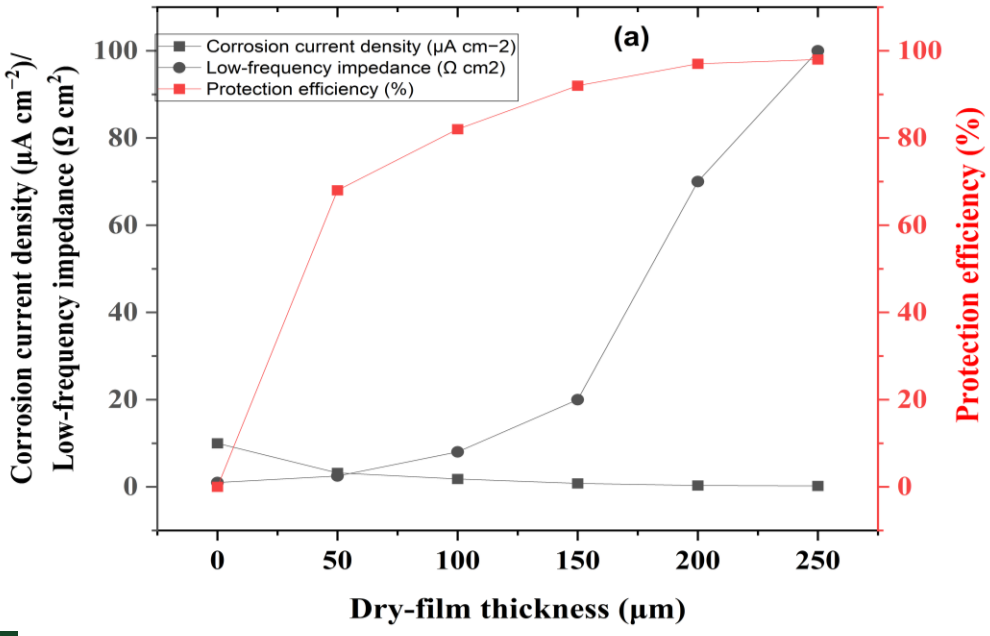


Fig. 1(a). Effect of dry-film thickness on the corrosion current density, low-frequency impedance, and corrosion-protection efficiency of silica-reinforced epoxy-coated mild steel

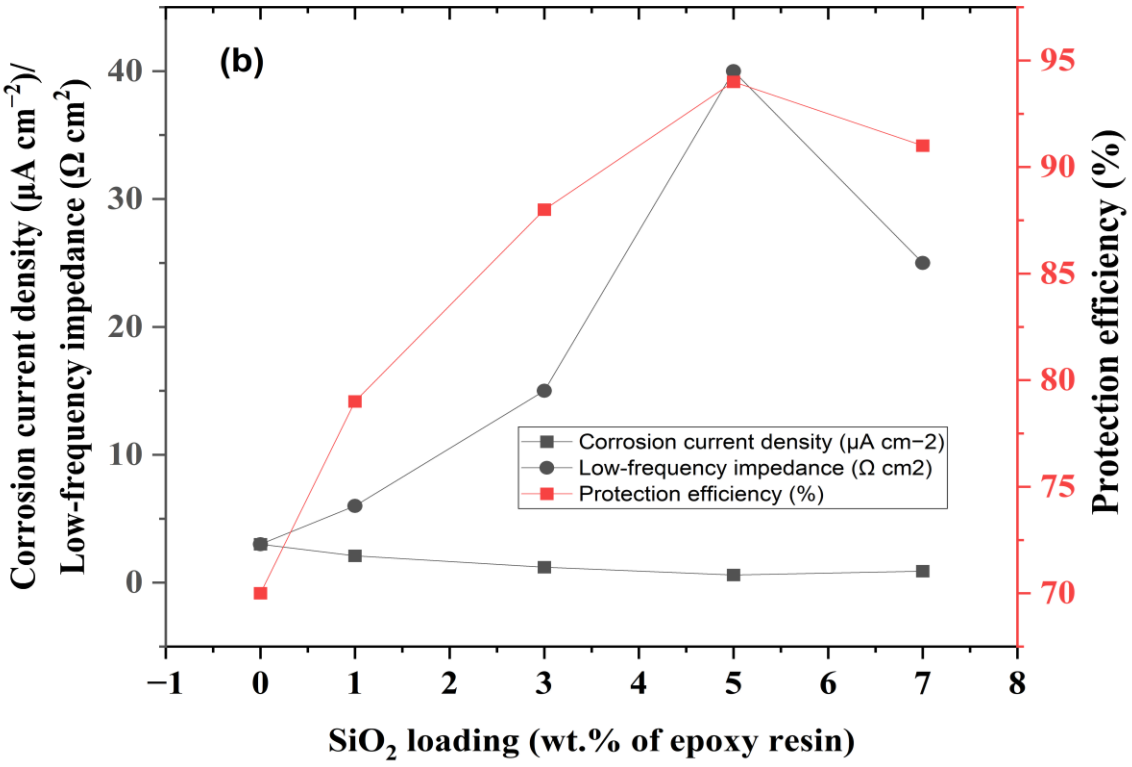


Fig. 1(b). Effect of SiO_2 nanoparticle loading on the corrosion current density, low-frequency impedance, and corrosion-protection efficiency of epoxy-coated mild steel.

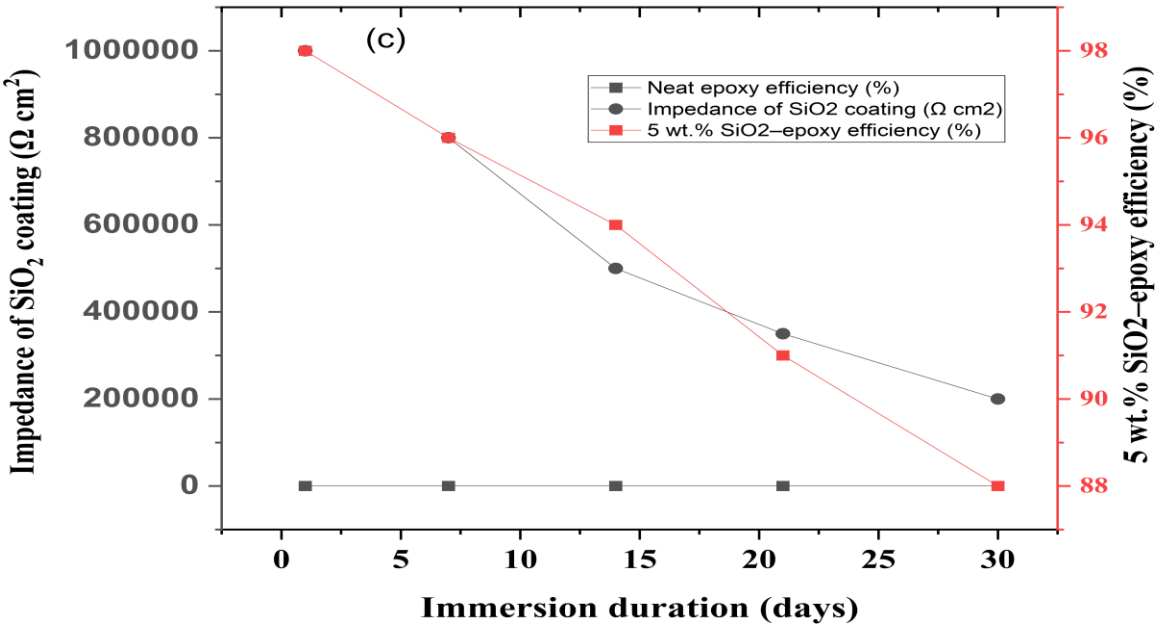


Fig. 1(c). Effect of immersion duration on the corrosion-protection efficiency and low-frequency impedance of neat epoxy and 5 wt.% SiO_2-reinforced epoxy coatings.

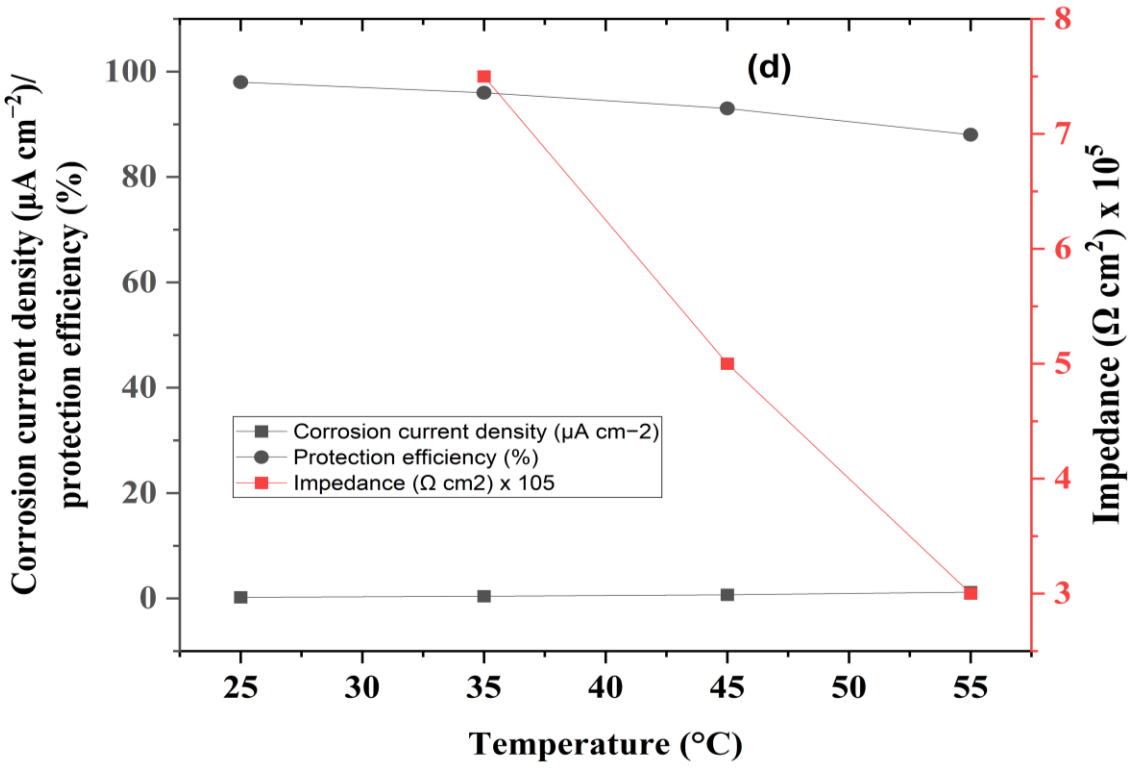


Fig. 1(d). Effect of solution temperature on the corrosion current density, corrosion-protection efficiency, and impedance of silica-reinforced epoxy-coated mild steel.

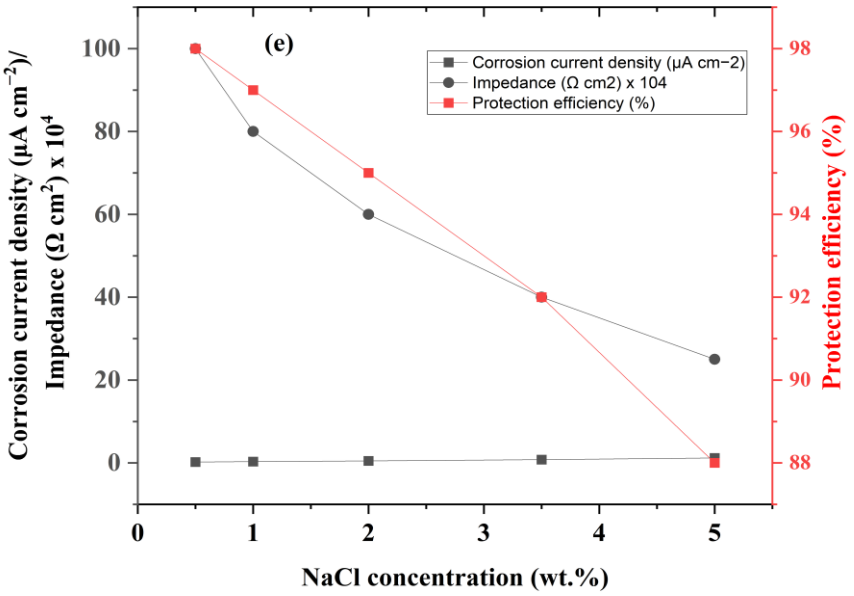


Fig. 1(e). Effect of NaCl concentration on the corrosion current density, low-frequency impedance, and corrosion-protection efficiency of silica-reinforced epoxy-coated mild steel

Fig. 1(a) illustrates the influence of dry-film thickness on the corrosion-protection performance of the silica-reinforced epoxy coating. The protection efficiency increases from approximately 0% for the uncoated control to 68%, 82%, 92%, 97%, and 98% at coating thicknesses of 50, 100, 150, 200, and 250 µm, respectively. Over the same thickness range, the corrosion current density decreases, while low-frequency impedance increases.

The relationship between corrosion current density and protection efficiency is expressed by equation 2 Akpanudo, 2026)

$$\%\eta = \left(1 - \frac{i_{corr,c}}{i_{corr,uc}}\right) \times \frac{100}{1} \qquad (2)$$

where $i_{corr,c}$ and $i_{corr,uc}$ are the corrosion current densities of coated and uncoated steel, respectively. The results obtained are shown in Table 2. These results indicate that increasing the coating thickness substantially improves the corrosion-protection performance within the investigated range. The reduction in corrosion current density suggests that the coating limits electrochemical reactions at the steel surface, while the increase in impedance indicates a more effective barrier against electrolyte penetration.

The percentage increase in impedance between the 50 and 250 µm coatings was calculated using equation 3 (Eddy *et al*., 2022)

$$Z\ (\%) = \left(\frac{Z_{250} - Z_{50}}{Z_{50}}\right) \times \frac{100}{1} \qquad (3)$$

The results obtained are also recorded in Table 2. From the results, it is observed that the impedance increases by 3900%, corresponding to a 40-fold increase. This behaviour is consistent with the barrier-protection mechanisms of organic coatings described by Sørensen et al. (2009).

The implication is that increasing coating thickness can improve the durability of steel structures exposed to chloride-containing environments. Nevertheless, the 250 µm coating should be regarded as the best-performing thickness among those tested, rather than automatically being the most economical or practical choice. Adhesion, curing, cracking, and material consumption should also be considered.

Table 2. Effect of dry-film thickness on corrosion-protection performance of silica-reinforced epoxy coating on mild steel

Dry-film thickness (μm)	Corrosion current density, i_{corr} (μA cm⁻²)	Protection efficiency, η (%)	Low-frequency impedance, |Z| (Ω cm²)	Impedance increase relative to 50 μm (%)
Uncoated control	10.00	0.0	1,000	—
50	3.20	68.0	25,000	0.0
100	1.80	82.0	80,000	220.0
150	0.80	92.0	200,000	700.0
200	0.30	97.0	700,000	2,700.0
250	0.20	98.0	1,000,000	3,900.0

Fig. 1(b) shows the effect of silica nanoparticle loading on the electrochemical performance of the epoxy coating. Protection efficiency increases from 70% for neat epoxy to 79%, 88%, and 94% at 1, 3, and 5 wt.% SiO_2, respectively. However, increasing the loading to 7 wt.% reduces the efficiency to approximately 91%. The corrosion current density follows the opposite trend, decreasing from 3.00 for neat epoxy to 0.60 at 5 wt.% SiO_2 before increasing to 0.90 at 7 wt.%. The impedance curve similarly reaches its maximum at 5 wt.% loading before declining at 7 wt.% (Table 3).

Table 3. Effect of SiO_2 nanoparticle loading on the corrosion-protection performance of epoxy-coated mild steel

SiO_2 loading (wt.% of epoxy resin)	Corrosion current density, i_{corr} (μA cm⁻²)	Protection efficiency (%)	Low-frequency impedance, |Z| (Ω cm²)	Impedance change relative to 5 wt.% (%)
0 (neat epoxy)	3.00	70.0	30,000	−92.5
1	2.10	79.0	60,000	−85.0
3	1.20	88.0	150,000	−62.5
5	0.60	94.0	400,000	0.0
7	0.90	91.0	250,000	−37.5

The 5 wt.% SiO_2 coating exhibited the highest protection efficiency (94%) and low-frequency impedance (400,000 Ω cm²), together with the lowest corrosion current density (0.60 μA cm⁻²). Increasing the silica loading to 7 wt.% reduced protection efficiency to 91% and impedance to 250,000 Ω cm², representing a 37.5% decrease in impedance relative to the 5 wt.% formulation.

These results suggest that an optimum silica concentration may improve the barrier properties of epoxy coatings, whereas excessive loading may compromise performance through particle agglomeration or coating defects. Therefore, 5 wt.% SiO_2 is the best-performing formulation among the concentrations investigated, subject to experimental validation.

Fig. 1(c) illustrates the effect of immersion duration on the corrosion-protection performance of neat epoxy and 5 wt.% SiO_2-reinforced epoxy coatings on mild steel. The corresponding numerical results and calculated parameters are presented in Table 4. The protection efficiency of the silica-reinforced coating decreases from 98% after 1 day to 96%, 94%, 91%, and 88% after 7, 14, 21, and 30 days, respectively. Over the same period, the low-frequency impedance decreases from 1.0×10^6 to 2.0×10^5 Ω cm^2. The retention of protection efficiency was calculated relative to the initial value using equation 4:

$$R_\eta(\%) = \frac{\eta_t}{\eta_0} \times \frac{100}{1} \quad (4)$$

where η_t is the protection efficiency at time and η_0 is the initial protection efficiency.

For the 30-day immersion period, the retention is 89.80% (Table 4). This indicates that the final protection-efficiency value represents 89.80% of the initial value, although the absolute protection efficiency after 30 days is 88%.

The retention of low-frequency impedance was calculated using equation 5 (Piccardi *et al.*, 2025),

$$R_Z(\%) = \frac{Z_t}{Z_0} \times \frac{100}{1} \quad (5)$$

where Z_t is the impedance at the specified immersion duration and Z_0 is the impedance at the initial measurement. At 30 days, R_Z was calculated as 20.0%. The calculated values and the corresponding changes in performance are summarized in Table 4.

Table 4 shows that the silica-reinforced coating maintains higher protection efficiency than neat epoxy throughout the 30-day exposure period. After 30 days, the difference between the two coatings is 20 percentage points (88% compared with 68%). However, the impedance of the silica-reinforced coating declines by 80% over this period, suggesting a substantial deterioration in its barrier response despite its relatively high remaining protection efficiency. The declining impedance may reflect water absorption, electrolyte penetration through coating defects, or changes at the steel–coating interface.

These mechanisms require confirmation through measured EIS spectra, adhesion tests, and post-immersion surface examination. The results suggest that silica reinforcement may help maintain protection during prolonged exposure, but longer-term testing is necessary to establish durability.

Table 4. Effect of immersion duration on corrosion-protection performance of neat epoxy and 5 wt.% SiO_2-reinforced epoxy coatings

Immersion duration (days)	Neat epoxy efficiency (%)	SiO_2–epoxy efficiency (%)	Impedance (Ω cm²)	Efficiency retention (%)	Impedance retention (%)	Impedance loss relative to day 1 (%)
1	82	98	1,000,000	100.00	100.00	0.00
7	78	96	800,000	97.96	80.00	20.00
14	74	94	500,000	95.92	50.00	50.00
21	71	91	350,000	92.86	35.00	65.00
30	68	88	200,000	89.80	20.00	80.00

Fig. 1(d) illustrates the influence of solution temperature on the corrosion-protection performance of the silica-reinforced epoxy coating. The protection efficiency decreases from 98% at 25 °C to 96%, 93%, and 88% at 35, 45, and 55 °C, respectively. Over the same temperature range, impedance decreases from

1.0×10^6 Ω cm^2, while corrosion current density increases from 0.20 to 1.20 μA cm^{-2}.

The absolute change in protection efficiency was calculated using equation 6, and the result was 10%.

$$\Delta\eta = \eta_{25} - \eta_{55} \quad (6)$$

The relative impedance decrease was calculated using equation 7:

$$\Delta Z(\%) = \frac{Z_{25}=Z_{55}}{Z_{25}} \times \frac{100}{1} \quad (7)$$

The relative increase in corrosion current density was also calculated using equation 8:

$$\Delta i = \frac{i_{55}-i_{25}}{i_{55}} \times \frac{100}{1} \quad (8)$$

The calculated results based on the different equations (equations 6 to 8) are summarized in Table 5.

Table 5. Effect of solution temperature on corrosion-protection performance of SiO_2-reinforced epoxy-coated mild steel

Karabatsos, G. J.; Hsi, N. Structural Studies by Nuclear Magnetic Resonance. XI. Conformations and Configurations of Oxime O-Methyl Ethers. *Tetrahedron* **1967**.

Temperature (°C)	Corrosion current density (μA cm^{-2})	Protection efficiency (%)	Impedance (Ω cm^2)	Efficiency decrease from 25 °C (percentage points)	Impedance decrease from 25 °C (%)
25	0.20	98	1,000,000	0	0
35	0.40	96	750,000	2	25
45	0.70	93	500,000	5	50
55	1.20	88	300,000	10	70

As shown in Table 5, increasing temperature is accompanied by a progressive reduction in protection efficiency and impedance. The 500% increase in corrosion current density between 25 and 55 °C suggests a substantial increase in electrochemical activity under the higher-temperature condition. Higher temperatures may accelerate electrolyte transport through the coating and electrochemical reactions at coating defects. Temperature can also alter polymer permeability and the properties of the coating–steel interface.

The decrease in impedance is consistent with a deterioration in the coating's barrier response. Nevertheless, temperature also affects electrolyte conductivity, so impedance changes should be interpreted using measurements taken at controlled temperatures and an appropriate equivalent-circuit model.

The results suggest that the coating performs best at 25 °C within the investigated range. For practical applications, its suitability for elevated-temperature environments should be assessed through controlled immersion tests, repeated EIS measurements, and post-exposure adhesion and surface examinations.

Fig. 1(e) shows the effect of NaCl concentration on the electrochemical performance of the silica-reinforced epoxy coating. Protection efficiency decreases from 98% at 0.5 wt.% NaCl to 97%, 95%, 92%, and 88% at 1, 2, 3.5, and 5 wt.% NaCl, respectively. The impedance also decreases with increasing salt concentration, while corrosion current density increases.

The absolute decrease in protection efficiency between the lowest and highest concentrations was calculated using equation 9, while the relative impedance decrease and the relative increase in corrosion current density were calculated based on equations 10 and 11, respectively (Akpanudo, 2026)

$$\Delta\eta = \eta_{0.5} - \eta_{5.0} \quad (9)$$

$$\Delta Z(\%) = \frac{Z_{0.5} - Z_{5.0}}{Z_{0.5}} \times \frac{100}{1} \quad (10)$$

$$\Delta i(\%) = \frac{i_{.5.0} - i_{0.5}}{i_{0.5}} \times \frac{100}{1} \quad (11)$$

The results obtained from equations 9 to 11 are summarized in Table 6.

Table 6. Effect of NaCl concentration on corrosion-protection performance of SiO_2-reinforced epoxy-coated mild steel

NaCl concentration (wt.%)	Corrosion current density (μA cm^{-2})	Protection efficiency (%)	Impedance (Ω cm^2)	Efficiency decrease from 0.5 wt.% (percentage points)	Impedance decrease from 0.5 wt.% (%)
0.5	0.20	98	1,000,000	0	0
1.0	0.30	97	800,000	1	20
2.0	0.50	95	600,000	3	40
3.5	0.80	92	400,000	6	60
5.0	1.20	88	250,000	10	75

Table 6 reveals a progressive decline in corrosion-protection performance as NaCl concentration increases. The impedance decreases by 75%, while the corrosion current density increases by 500% between 0.5 and 5 wt.% NaCl. These changes suggest that the coating's electrochemical barrier response becomes less effective under increasingly aggressive saline conditions.

Chloride ions can promote localized corrosion at coating defects and exposed areas of steel. Increased electrolyte concentration also changes solution conductivity, which may affect the measured impedance. Consequently, the results are consistent with deteriorating barrier performance but do not, by themselves, prove the precise mechanism of chloride penetration.

The implication is that coating performance should be evaluated under the salinity expected in its intended service environment. The 98% efficiency at 0.5 wt.% NaCl should not be assumed to apply under more concentrated saline conditions.

The results in Tables 2–6 indicate that coating thickness, silica loading, immersion duration, temperature, and NaCl concentration influence the corrosion-protection performance of silica-reinforced epoxy coatings.

The best-performing conditions in the individual comparisons were a dry-film thickness of 250 μm, a silica loading of 5 wt.% SiO_2, a one-day immersion period, a temperature of 25 °C, and a NaCl concentration of 0.5 wt.%. The highest illustrative protection efficiency was 98%, while the lowest was 68% for the 50 μm coating.

These conditions were evaluated separately. Therefore, the results do not establish that combining the 250 μm thickness and 5 wt.% silica loading will necessarily yield 98% protection efficiency under all environmental conditions. A factorial experimental design is required to evaluate interactions between coating thickness, silica loading, and exposure conditions.

Low-frequency impedance provides complementary evidence of barrier performance but should not be substituted directly into this equation. Actual experimental results should include replicate measurements, mean and standard deviation, suitable statistical comparisons, and consistent axis scaling in the electrochemical plots.

4.0 Conclusion

This study investigated the corrosion-protection performance of silica (SiO_2) nanoparticle-reinforced epoxy coatings on mild steel under different experimental conditions, including dry-film thickness, silica loading, immersion duration, solution temperature, and sodium chloride concentration. The results indicate that coating thickness and silica content are important factors influencing corrosion resistance. Increasing the dry-film thickness from 50 to 250 µm increased the illustrative protection efficiency from 68% to 98%, accompanied by a substantial increase in low-frequency impedance and a reduction in corrosion current density. Similarly, increasing the silica loading improved protection efficiency up to 5 wt.%, at which an efficiency of 94% was obtained, while further increasing the loading to 7 wt.% reduced the efficiency to 91%. This behaviour suggests that excessive nanoparticle loading may compromise coating performance through agglomeration or defects in the polymer matrix.

The environmental exposure results further indicate that prolonged immersion, elevated temperature, and increasing NaCl concentration may reduce the coating's protective performance. After 30 days of immersion, the 5 wt.% SiO_2-reinforced epoxy coating retained an illustrative protection efficiency of 88%, compared with 68% for neat epoxy. Increasing the temperature from 25 to 55 °C and the NaCl concentration from 0.5 to 5.0 wt.% reduced the respective protection efficiencies from 98% to 88%. These trends highlight the importance of evaluating coatings under realistic operating conditions rather than relying solely on initial corrosion-resistance measurements.

Overall, a dry-film thickness of 250 µm and a silica loading of 5 wt.% represent promising conditions for further investigation. However, these conditions were assessed separately, and their combined performance requires experimental verification. Because the numerical results used in this manuscript are illustrative rather than measured laboratory data, the reported efficiencies and optimum conditions should be regarded as preliminary hypotheses. Experimental validation using potentiodynamic polarization, electrochemical impedance spectroscopy, coating-adhesion testing, and post-exposure surface characterization is necessary to establish the actual performance and durability of the coating. Such validation will provide a sound basis for assessing the suitability of silica-reinforced epoxy coatings for corrosion protection of mild steel in marine and other chloride-containing environments.

5.0 References

Akpanudo, N. W. (2026). Electrochemical performance and corrosion protection of zinc–carbon quantum dot (Zn–CQD) nanocomposite coatings on mild steel. *Communication in Physical Sciences*, 13, 7, pp. 1116–1138.

Alam, M. A., Samad, U. A., Sherif, E.-S. M., Poulose, A. M., Mohammed, J. A., Alharthi, N., & Al-Zahrani, S. M. (2020). Influence of SiO_2 content and exposure periods on the anticorrosion behavior of epoxy nanocomposite coatings. *Coatings*, 10, 2, Article 118. https://doi.org/10.3390/coatings10020118

Ameh, P. O., & Eddy, N. O. (2016). Theoretical and experimental studies on the corrosion inhibition potentials of 3-nitrobenzoic acid for mild steel in 0.1 M H_2SO_4. *Cogent Chemistry*, 2, 1, pp. 1–18.

ASTM International. (2017). *Standard test method for measurement of dry film thickness of nonmagnetic coatings applied to ferrous metals and nonmagnetic, nonconductive coatings applied to non-ferrous metals* (ASTM Standard D7091-13). https://doi.org/10.1520/D7091-13

ASTM International. (2020). Standard test method for pull-off strength of coatings using portable adhesion testers (ASTM Standard D4541-17). https://doi.org/10.1520/D4541-17

Bharadwaj, R. K. (2001). Modeling the barrier properties of polymer-layered silicate nanocomposites. *Macromolecules,* 34, 26, pp. 9189–9192. https://doi.org/10.1021/ma010780b

Eddy, N. O. (2010). Adsorption and inhibitive properties of ethanol extract of Garcinia kola & Cola nitida for the corrosion of mild steel in H_2SO_4. *Pigment & Resin Technology,* 39, 6, pp. 348–354.

Eddy, N. O. (2011). Experimental and theoretical studies on the inhibition potentials of some derivatives of cyclopenta-1,3-diene for the corrosion of mild steel in HCl solutions. *International Journal of Quantum Chemistry,* 111, 14, pp. 3456–3474.

Eddy, N. O., Ameh, P. O., Anduang, O. O., & Emaikwu, V. (2014). Chemical information from GCMS & FTIR studies on Ficus thonningii gum & its potential as a corrosion inhibitor for aluminium in acidic medium. International *Journal of Chemical Material and Environmental Research*, 1, 1, pp. 3–15.

Eddy, N. O., Ekwumemgbo, P., & Odoemelam, S. A. (2008). Inhibition of the corrosion of mild steel in H_2SO_4 by 5-amino-1-cyclopropyl-7-[(3R, 5S)-3,5-dimethylpiperazin-1-yl]-6,8-difluoro-4-oxo-quinoline-3-carboxylic acid (ACPDQC). *International Journal of Physical Sciences,* 3, 11, pp. 275–280.

Eddy, N. O., Odoemelam, S. A., & Akpanudoh, N. W. (2008). Synergistic effect of amoxicillin & halides on the inhibition of the corrosion of mild steel in H_2SO_4. *Journal of Pure and Applied Science*, 4, 12, pp. 1963–1973.

Eddy, N. O., Odoemelam, S. A., Ogoko, E. C., Ukpe, R. A., Garg, R., & Anand, B. (2022). Experimental and quantum chemical studies of synergistic enhancement of the corrosion inhibition efficiency of ethanol extract of Carica papaya peel for aluminum in solution of HCl. *Results in Chemistry*, 100290. https://doi.org/10.1016/j.rechem.2022.100290

Eddy, N. O., & Odiongenyi, A. O. (2008). Ethanol extract of Musa species peels as a green corrosion inhibitor for mild steel: Kinetics, adsorption & thermodynamic considerations. *Advances in Natural and Applied Sciences,* 2, 1, pp. 35–42.

Ghanbari, A., & Attar, M. M. (2015). A study on the anticorrosion performance of epoxy nanocomposite coatings containing epoxy-silane treated nano-silica on mild steel substrate. *Journal of Industrial and Engineering Chemistry,* 23, pp. 145–153. https://doi.org/10.1016/j.jiec.2014.08.008

Kickelbick, G. (2003). Concepts for the incorporation of inorganic building blocks into organic polymers on a nanoscale. *Progress in Polymer Science*, 28, 1, pp. 83–114. https://doi.org/10.1016/S0079-6700(02)00019-9

Mansfeld, F. (1990). Electrochemical impedance spectroscopy (EIS) as a new tool for investigating methods of corrosion protection. *Electrochimica Acta*, 35, 10, pp. 1533–1544. https://doi.org/10.1016/0013-4686(90)80007-B

Odoemelam, S. A., & Eddy, N. O. (2008). Effect of pyridoxal hydrochloride-2,4-dinitrophenyl hydrazone on the corrosion of mild steel in HCl. *Journal of Surface Science and Technology*, 24, 1, p. 2.

Odoemelam, S. A., & Eddy, N. O. (2009). Inhibition of the corrosion of zinc in H_2SO_4 by 9-deoxy-9a-aza-9a-methyl-9a-homoerythromycin A (azithromycin). *Portugaliae Electrochimica Acta*, 27, 1, pp. 57–68.

Piccardi, A., Pettinato, S., Rossi, M. C., Girolami, M., & Salvatori, S. (2025). Low-frequency measurements in electrochemical impedance spectroscopy: A brief review. *Electronics*, 14, 20, Article 4048. https://doi.org/10.3390/electronics14204048

Revie, R. W., & Uhlig, H. H. (2008*). Corrosion and corrosion control: An introduction to corrosion science and engineering* (4th ed.). John Wiley & Sons.

Sørensen, P. A., Kiil, S., Dam-Johansen, K., & Weinell, C. E. (2009). Anticorrosive coatings: A review. *Journal of Coatings Technology and Research*, 6, pp. 135–176. https://doi.org/10.1007/s11998-008-9144-2

Walter, G. W. (1986). A review of impedance plot methods used for corrosion performance analysis of painted metals. *Corrosion Science*, 26, 9, pp. 681–703. https://doi.org/10.1016/0010-938X(86)90033-8

Declarations

Funding

The author declared no external sources kf funding

Conflict of Interest

The author declared no conflict of interest

Data Availability

Data shall be made available upon request

Ethical Considerations

Not applicable

Author Contributions

The author carried out all components of the work.